

# FLOW SIMULATION AND PERFORMANCE PREDICTION OF CENTRIFUGAL PUMPS USING CFD-TOOL

Abdulkadir Aman, Sileshi Kore and Edessa Dribssa\*

Department of Mechanical Engineering  
Addis Ababa Institute of Technology, Addis Ababa University

## ABSTRACT

*With the aid of computational fluid dynamics, the complex internal flows in water pump impellers can be well predicted, thus facilitating the product development process of pumps. In this paper a commercial CFD code was used to solve the governing equations of the flow field. A 2-D simulation of turbulent fluid flow is presented to visualize the flow in a centrifugal pump, including the pressure and velocity distributions. The standard  $k-\epsilon$  turbulence model and SIMPLEC algorithm were chosen for turbulence model and pressure-velocity coupling respectively. The simulation was steady and moving reference frame was used to consider the impeller-volute interaction. The head and efficiency at different flow rates are predicted and they agree well with those available in literature for similar pump. From the simulation results it was observed that the flow change has an important effect on the location and area of low pressure region behind the blade inlet and the direction of velocity at impeller inlet. From the study it was observed that FLUENT simulation results give good prediction of performance of centrifugal pump and may help to reduce the required experimental work for the study of centrifugal pump performance.*

**Keywords:** Centrifugal Pump, FLUENT, Performance prediction, CFD

## INTRODUCTION

A centrifugal pump is one of the machines commonly used in industrial plants to raise the energy content of a liquid flowing through it. It does so by converting energy of a prime mover (an electric motor or turbine) first into velocity or kinetic energy, and then into pressure energy of a liquid that is being pumped. The energy changes occur by virtue of two main parts of the pump, the impeller and the volute or diffuser. The impeller is the rotating part that converts driver energy into the kinetic energy. The volute or diffuser is the

stationary part that transforms the kinetic energy of the liquid into pressure energy.

Centrifugal pumps are prevalent for many different applications in the industrial and other sectors. Nevertheless, their design and performance prediction process is still a difficult task, mainly due to the great number of free geometric parameters involved. On the other hand the significant cost and time of the trial-and-error process by constructing and testing physical prototypes reduces the profit margins of the pump manufacturers. For this reason, CFD analysis is currently being used in hydrodynamic design for many different pump types [1].

Over the past few years, with the rapid development of the computer technology and computational fluid dynamics (CFD), numerical simulation, like academic analysis and experimental research, has become an important tool to study flow field in pumps and predict pump performance [2]. Numerical simulation makes it possible to visualize the flow condition inside a centrifugal pump, and provides valuable information to centrifugal pump's hydraulic design [3].

Despite the great progress in recent years, even CFD analysis remains rather expensive for the industry, and the need for faster mesh generators and solvers is imperative [1].

## GOVERNING EQUATIONS

Since the fluid surrounding the impeller rotates around the axis of the pump the fundamental equations of fluid dynamics must be organized in two reference frames, stationary and rotating reference frames. To accomplish this, the Multiple Reference Frame (MRF) model has been used. The basic idea of the model is to simplify the flow inside the pump into an instantaneous flow at one position, to solve unsteady-state problem with steady-state method [3]. In this approach, the governing equations are set in a rotating reference

\* E-mail: [Edessa\\_dribssa@yahoo.com](mailto:Edessa_dribssa@yahoo.com)

frame, and coriolis and centrifugal forces are added as source terms. The mass conservation and momentum equations for a rotating reference frame are as follows.

Mass conservation:

$$\nabla \cdot (\rho \vec{v}_r) = 0 \tag{1}$$

Conservation of angular momentum:

$$\nabla \cdot (\rho \vec{v}_r \vec{v}) + \rho (\vec{\omega} \times \vec{v}) = -\nabla p + \nabla \vec{\tau} \tag{2}$$

Where:

- $\vec{v}_r$  is the relative velocity
- $\vec{v}$  is the absolute velocity
- $\vec{\omega}$  is the angular velocity

The fluid velocities can be transformed from the stationary frame to the rotating frame using the following relation:

$$\vec{v}_r = \vec{v} - \vec{u}_r \tag{3}$$

$$\vec{u}_r = \vec{\omega} \times \vec{r} \tag{4}$$

Where:

- $\vec{u}_r$  is the whirl velocity (the velocity viewed due to the moving frame) and
- $\vec{r}$  is the position vector from the origin of the rotating frame.

### DESCRIPTION OF THE MODEL

The model geometry is complex and asymmetric due to the blade and volute shape. The GAMBIT package was used to build the geometry, to generate meshes and set up boundary zones of the centrifugal pump model for the CFD simulation analysis. The model contains six impeller blades spaced 60° between them. A triangular mesh was selected for meshing the flow domain. The impeller has an outlet diameter of 124 mm and inlet diameter of 52 mm. The eye diameter is 20mm. the model is divided into three boundary zone types (inlet, impeller and volute). A view of the generated grid of the centrifugal pump considered for this study is shown in Fig. 1.

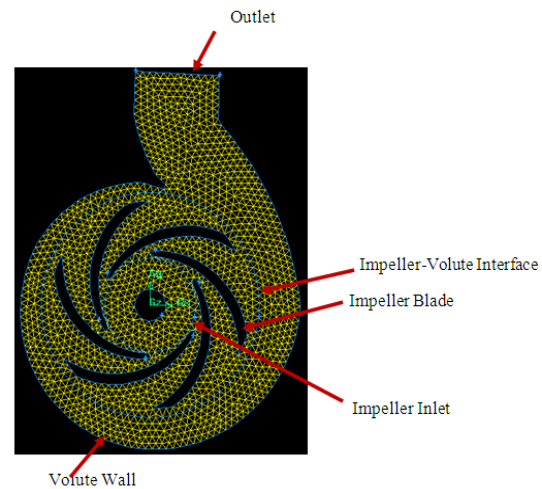


Figure 1 2-D model of centrifugal pump after meshing.

The mesh file contains the coordinates of all the nodes, connectivity information that tells how the nodes are connected to one another to form faces and cells, and zone types and number of all the faces. The grid file does not contain any boundary conditions, flow parameters, or solution parameters. It is an intermediate step in the overall process of creating a usable model which is exported, as a mesh file, to be read in FLUENT.

### COMPUTATIONAL METHOD AND BOUNDARY CONDITIONS

In order to calculate the flow field in the vane and channel of the casing a commercial CFD code, FLUENT, was used. The governing integral equations for the conservation of mass and momentum were discretized using finite volume method. Then, standard k-ε model was adapted for turbulence calculation, from the three known k-ε models (Standard k-ε, RNG k-ε and Realizable k-ε). The standard k-ε model is a semi-empirical model based on model transport equations for the turbulence kinetic energy (k) and its dissipation rate (ε). The model transport equation for k is derived from the exact equation, while the model transport equation for ε was obtained using physical reasoning and bears little resemblance to its mathematically exact counterpart [4].

Two numerical solvers of segregated and coupled employ a similar discretization process, but the approach used for linearizing and solving the discretized equations is different. The segregated solver solves the governing equations sequentially, while the coupled solves them simultaneously [1]. In the present analysis, the segregated solver was used since the coupled solver is usually used in high compressible flows in which the flow and energy equations are coupled.

The pressure-velocity coupling methods recommended for steady-state calculations are SIMPLE or SIMPLC [1, 5, 6]. For the present simulation SIMPLC algorithm was preferred due to its high convergence rate. Second order upwind scheme was employed for discretization for equations of momentum, turbulent kinetic energy and turbulent dissipation rate.

Velocity-inlet boundary condition was imposed on pump inlet position. It was specified to be normal to the boundary and it is defined with reference to the absolute frame. The turbulence intensity for all conditions is considered 1%. Out flow boundary condition was imposed at outlet with a flow rate weighting of 1.

Outer walls were stationary but the inner walls were rotational. There were interfaces between the stationary and rotational regions. Also non-slip boundary conditions have been imposed over the impeller blades and walls, the volute casing and the inlet wall. A constant angular velocity of 2900 rpm was imposed for rotating fluid.

**RESULTS AND DISCUSSION**

**Pressure Distribution**

The contour plot of variation of Static Pressure is shown in Fig. 2. It can be seen from the figure that, static pressure inside impeller and volute is asymmetry distributed. The maximum static pressure area appears at volute tongue and outlet regions and the minimum one at the back of blade at impeller inlet region.

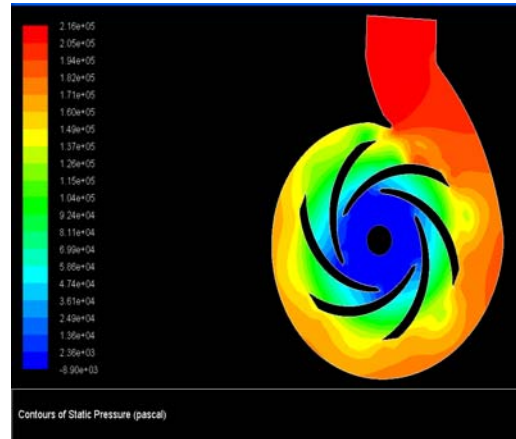


Figure 2 Contours of static pressure (Pascal)

It can also be observed from the figure that, the pressure increases gradually from impeller inlet to outlet. The static pressure on pressure side is evidently larger than that on suction side at the same impeller radius. The lowest static pressure (-89000 Pa) inside pump appears in suction surface at the impeller inlet, the position where cavitation often appears inside the pump.

The variation of static pressure with flow rate is also shown in Fig. 3. As the flow rate goes on increasing the pressure gradually lowers. As can be seen from Fig. 3, there is an obvious low pressure area at the suction side of the blade inlet at small flow rate, as the flow increases the area gets close to the middle of the blade suction side.

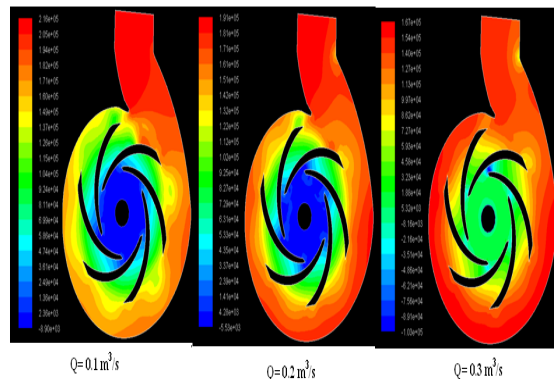


Figure 3 Variation of static pressure at different flow rates

### Velocity Distribution

The contour plot of absolute velocity distribution is shown in Fig. 4. As shown in the figure, the velocity increases from impeller inlet to outlet and reaches a peak value of 21.1 m/s at impeller outlet. After entering the volute, the velocity begins to fall down, reaching the lowest at the outlet region inside the volute.

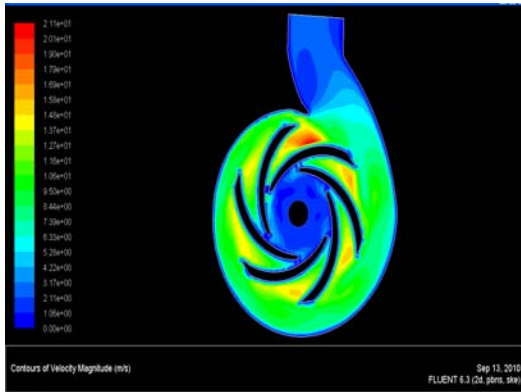


Figure 4 Contours of absolute velocity magnitude (m/s)

The contour plot of the tangential component of the absolute velocity is also shown in Fig. 5. As expected, the tangential velocity reaches its peak at impeller outlet. It starts to fall after entering the volute and reaches the lowest at the outlet region of the volute.

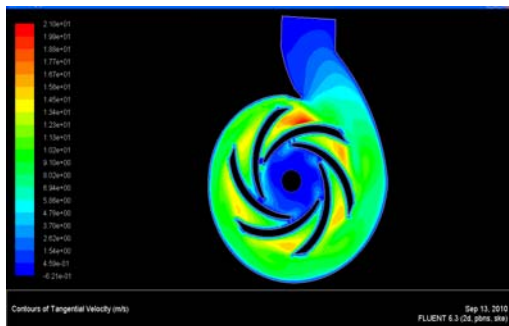


Figure 5 Contours of tangential component of the absolute velocity (m/s)

Figure 6 shows velocity vectors colored by velocity magnitude. As can be seen from the figure the velocity is higher at impeller outlet and lower at impeller inlet and volute outlet. It can be seen clearly how the velocity goes on decreasing from volute inlet to outlet.

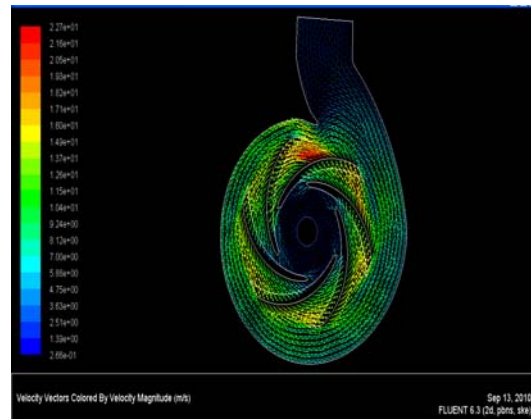


Figure 6 Absolute velocity vectors colored by velocity magnitude

### Validation

In order to validate the analysis, the simulation results of flow rate at outer circumference of the impeller are compared with analytical formula used to compute the volume flow rate at impeller outlet. The volume flow rate is given by:

$$Q = 2\pi r_2 b_2 C_{2r} \quad (5)$$

Where:

$r_2$  is the outer radius of the impeller

$b_2$  is thickness of flow passage at the outer circumference.

$C_{2r}$  is the radial component of the absolute velocity at the outer circumference of the impeller.

The outer radius and thickness of flow passage for each design flow rate are 0.062m and unit thickness respectively.

The comparison between the design flow rate used for simulation and the flow rate obtained using the analytical formula is summarized in Table 1.

Table 1: Comparison of results of volume flow rate obtained from simulation and analytical formula.

| Design flow rate (m <sup>3</sup> /s) | Radial velocity at impeller outlet, C <sub>2r</sub> (m/s) | Flow rate computed using analytical formula (Eq. (5)) (m <sup>3</sup> /s) | Percentage error (%) |
|--------------------------------------|---|---|----------------------|
| 0.1                                  | 0.2535  | 0.09876   | 1.24                 |
| 0.2                                  | 0.5123  | 0.19957   | 0.215                |
| 0.3                                  | 0.76511   | 0.29805   | 0.650                |

As can be seen from the above table the analytical result gives a result which is very accurate and the percentage error is less than 1.25%. This shows the accuracy of both the analytical result and the CFD tool Fluent.

Generally the variation of velocity and pressure obtained in this analysis are consistent with theoretical concept and experimental values in pump analysis. Besides, the contour plots are similar to that obtained for similar pump analysis by different authors. Shujia and Baolin [2], obtained similar results in their virtual performance experiment of centrifugal pump using CFD.

**Performance Curves of Centrifugal Pumps**

The design parameters, i.e., Head Coefficient, Flow Coefficient, Power Coefficient and Hydraulic Efficiency are evaluated from the numerical output results of FLUENT. These parameters are used to compare the performance characteristics of different pump models [7]. The equations used to compute Head, Power and Efficiency are:

Head *H* is calculated by the following formula:

$$H = \frac{P_{out} - P_{in}}{\rho g}, \tag{6}$$

Where *p*<sub>out</sub> is the total pressure at pump outlet, *p*<sub>in</sub> is the total pressure at pump inlet, *ρ* is the density of liquid and *g* is the gravitational acceleration.

Hydraulic efficiency *η*<sub>h</sub> is calculated as:

$$\eta_h = \frac{\rho g H Q}{M \omega} \tag{7}$$

Where *M* is the impeller torque, *ω* is the angular velocity.

The water power is determined from the relationship [8]:

$$P = \rho g H Q \tag{8}$$

The operating characteristics are plotted after processing the numerical results from Fluent using Matlab.

Figure 7 shows the variation of head with flow rate. Theoretically it is expected that the head goes on decreasing as the flow rate increases for backward curved blades. Here also it can be seen from Fig.7 that, the head decreases with an increase in flow rate. The profile is similar to experimental results obtained for similar pump models by different authors [1, 3].

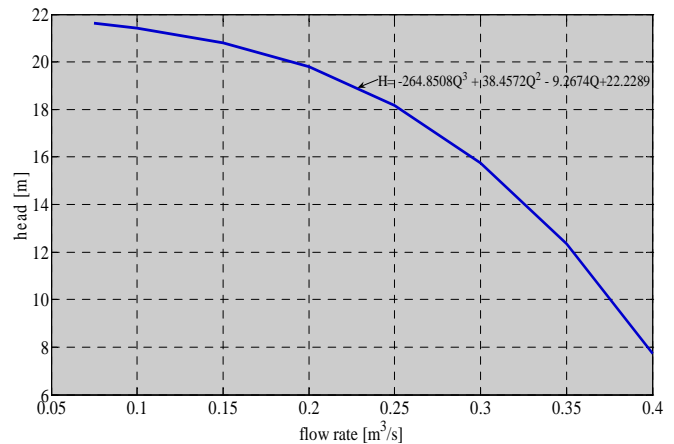


Figure 7 Pump head vs flow rate

Theoretically for an ideal case the head at design point is given by:

$$H = \frac{1}{g} [u_2 C_{2u} - u_1 C_{1u}] \quad (9)$$

Where:

$u_2$  and  $u_1$  are peripheral velocities of the rotor at outer and inner radius respectively.

$C_{2u}$  and  $C_{1u}$  are whirl components of the absolute velocity at outer and inner radius respectively.

At design point of the pump (point of maximum efficiency) which is  $0.25 \text{ m}^3/\text{s}$ , the magnitudes of velocity components are given below.

$C_{2u} = 9.665 \text{ m/s}$  and  $C_{1u} = 0.988 \text{ m/s}$  (obtained from simulation result)

$u_2 = 18.83 \text{ m/s}$  and  $u_1 = 7.896 \text{ m/s}$  (calculated,

$$u = \omega r)$$

Table 2 presents a comparison of the theoretical head and CFD result at design point

Table 2: Comparison of the theoretical head and CFD result at design point

| Design flow rate ( $\text{m}^3/\text{s}$ ) | Pump head obtained from simulation result (m) | Theoretical pump head obtained using analytical formula (Eq. (9)) (m) | Percentage Error (%) |
|--|---|---|----------------------|
| 0.25                                       | 19.05   | 17.76   | 6.77                 |

From Table 2, it can be seen that the theoretical head obtained using the analytical formula is close to the result obtained by simulation, with a percentage error of only 6.77%. Hence, it can be said that the CFD tool predicts well the pump head and the analytical formula also gives reasonably good result.

Figure 8 shows the variation of the fluid power with discharge. As shown in the figure, the power goes on increasing until it reaches a certain limit and then decreasing beyond a certain value of flow rate. The output power is maximum for a flow rate of  $0.3 \text{ m}^3/\text{s}$ .

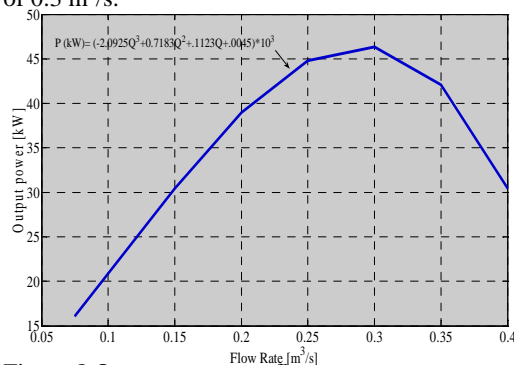


Figure 8 Output power vs. flow rate

Figure 9 shows the variation of hydraulic efficiency with flow rate. As can be seen from the figure, the point of maximum efficiency is  $0.25 \text{ m}^3/\text{s}$ .

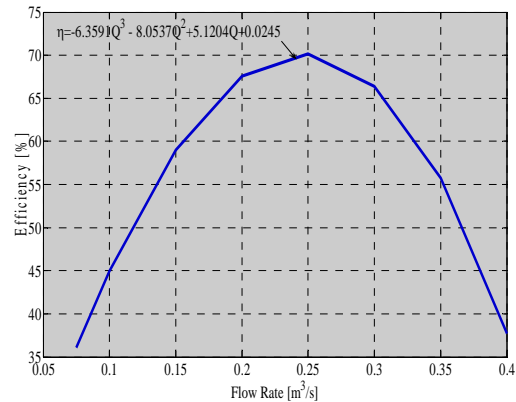


Figure 9 Efficiency Vs. flow rate curve for centrifugal pump

The optimum design flow rate for the pump considered for this study is  $0.25 \text{ m}^3/\text{s}$ . The variation of efficiency of the pump at design and off-design condition is similar to the experimental result for efficiency of the pump where the maximum efficiency is attained at design flow rate. Minggao and Shouqi [2] investigated experimentally and numerically a 6 bladed pump and obtained similar profile for efficiency variation with flow rate.

The pump head and efficiency curves are also shown in Fig. 10. The operating point of the pump can be selected by combining with the pump system curve. But from the graph it can be observed that, the flow rate - head combination of  $0.25 \text{ m}^3/\text{s}$  and 18 m gives the maximum efficiency.

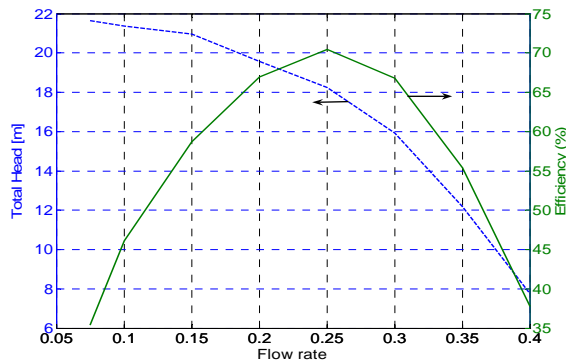


Figure 10 Pump head and efficiency vs. flow rate

### CONCLUSIONS

In this study, a steady state CFD analysis of a 2-D model of backward curved six bladed centrifugal pump is carried out. The contour and vector plot of pressure and velocity distributions in the flow passage are displayed. Besides, the operating characteristics of the pump are also computed from fluent numerical results.

Although specific experimental results are not available for the pump considered for this study, the results agree well with most of the available results obtained by different authors for a similar pump. From the study it was observed that there is a low pressure area at the suction side of blade inlet at small flow rate, as the flow increases, the area gets close to the middle of blade suction side. The static pressure also increases on diffusion section of the volute outlet markedly at small flow rate while the static pressure on the same place decreases at higher flow rate.

The simulation results for flow rate and head are also compared with analytical formulae used to predict the flow rate and theoretical head. There is a good agreement between the results and this also shows the accuracy of the analysis.

From the analysis it can be concluded that the flow pattern of a centrifugal pump can be described quite well with the moving reference frame (MRF) and the  $k-\epsilon$  Turbulence model. Moreover, valuable information to the pumps performance optimization can also be provided by analysis of numerical results from Fluent, which furthermore improves CFD based centrifugal pump design.

### REFERENCES

- [1] Jafarzadeh, B., Hajari, A., Alishahi, M.M. and Akbari, M.H., "The Flow Simulation of a Low-Specific-Speed High-Speed Centrifugal Pump", *Applied Mathematical Modeling*, vol. 35, 2011, pp. 242-249.
- [2] Minggao, T., Shouqi, Y., Houlin, L., Yong, W. and Kai, W., "Numerical Research on Performance Prediction for Centrifugal Pumps", *Chinese Journal of Mechanical Engineering*, Vol. 23, No. 1, 2010, pp. 1-6.
- [3] Shujia, Z., Baolin, Z., Qingbo, H. and Xianhua, L., "Virtual Performance Experiment of a Centrifugal Pump", *Proceedings of the 16th International Conference on Artificial Reality and Telexistence--Workshops (ICAT'06)*, 2006.
- [4] Fluent Inc.: FLUENT 6.3.2 Documentation – User's Guide, 2006.
- [5] Derakhshan, S. and Nourbakhsh, A., "Theoretical, Numerical and Experimental Investigation of Centrifugal Pumps in Reverse Operation", *Experimental Thermal and Fluid Science*, vol. 32, 2008, pp. 1620-1627.
- [6] Cheah, K.W., Lee, T. S., Winoto, S. H. and Zhao, Z.M., "Numerical Flow Simulation in a Centrifugal Pump at Design and Off-Design Conditions", *International Journal of Rotating Machinery*, Hindawi Publishing Corporation, Article ID 83641, 2007.
- [7] Derakhshan, S. and Nourbakhsh, A., "Experimental Study of Characteristic Curves of Centrifugal Pumps Working as Turbines in Different Specific Speeds", *Experimental Thermal and Fluid Science*, vol. 32, 2008, pp. 800-807.
- [8] Thin, K.H., Khaing, M.M. and Aye, K.M., "Design and Performance Analysis of Centrifugal Pump", *World Academy of Science, Engineering and Technology*, vol.46, 2008, pp. 422-429.